THE EXTENSION OF MINIMOS TO A THREE DIMENSIONAL SIMULATION PROGRAM

M. Thurner, S. Selberherr
Institut für Allgemeine Elektrotechnik und Elektronik
Technische Universität Wien
Gusshausstraße 27–29, A–1040 Wien, AUSTRIA

Abstract —An accurate three–dimensional simulaton program for MOSFET devices has been developed by extending MINIMOS (vers. 4) in 3D. The physical model is based on the 'hot-electron-transport-model', which includes the Poisson equation, the continuity equations and a selfconsistent set of equations for the currents, mobilities and carrier–temperatures. The standard finite difference discretization and the SOR (successive over relaxation) method are utilized to reduce computational time and memory requirements. Adaptive grid refinement is used to equidistribute the discretization errors. Three–dimensional effects like threshold shift for small channel devices, channel narrowing and the accumulation of carriers at the channel edge have been successfully modeled. Our analyses make clear that three–dimensional calculations are most important for accurate device modeling.

1 Introduction

Today's ULSI challenges new methods in device design. The present integrated circuits contain transistors of very small size whose operating characteristics depend upon highly three–dimensional structures. State of the art two–dimensional simulation programs cannot take into account any width effects which are of increasing importance for present and future ULSI MOS devices. Therefore we have extended the two–dimensional MINIMOS program to offer as additional feature hierarchical three–dimensional simulator capabilities. The purpose of this paper is to develop a three–dimensional model, to show the limitations of the two–dimensional approach, and to gain more physical insight by comparing the results of our 3D–model with two–dimensional results.

In section 2 we shall present briefly details of the physical model, the equations and the assumptions that the three–dimensional simulation program is based on.
The numerical methods and some mathematical investigations concerning the convergency of the solution are discussed in section 3.
Finally we present some results of our simulations and discuss it in section 4. An effect known from theory and from practical measurements, but not modeled until now, is presented there.

2 The physical model for the extension

The MOS transistor device structure as it has been simulated in three dimensions is shown in Fig. 1. The field oxide, which limits the channel width can be seen at the backside. The three–dimensional mathematical formulation is based on the set of the semiconductor equations.

$$div\ grad\ \psi = \frac{q}{\epsilon}(n - p - C) \tag{2.1}$$

$$div\ J_n = qR \tag{2.2}$$

$$div\ J_p = -qR \tag{2.3}$$

For the hot-electron-transport model [1] we write

$$J_n = -q\mu_n(n\ grad\ \psi - grad\ (U_{t_n} n)) \tag{2.4}$$

$$J_p = -q\mu_p(p\ grad\ \psi + grad\ (U_{t_p} p)) \tag{2.5}$$

$$U_t = U_{t_0} + \frac{2}{3}\tau_\epsilon v_{sat}^2\left(\frac{1}{\mu_{LISF}} - \frac{1}{\mu_{LIS}}\right) \tag{2.6}$$

τ_ϵ denotes the energy relaxation time which is assumed to be constant.
The function μ_{LIS} combines the mobility due to lattice and ionized impurity scattering with the influence of surface scattering yieling a cold carrier mobility. The mobility μ_{LIS} is then combined with the influence of the driving force F and the saturation velocity v_{sat} rsulting in the mobility μ_{LISF} of hot carriers.

In our simulations the Poisson equation (2.1) is always solved fully three–dimensional. For the first additional level of sophistication beyond the 2D hot-electron-transport model we assume negligible current flow in the direction of the channel width as natural simplification of the continuity equations (2.2 to 2.3).

$$J_{n_z} = J_{p_z} = 0$$

Assuming the validity of Boltzmann statistics the previously stated assumtion implies constant imrefs in the third direction:

$$\frac{\partial \varphi_n}{\partial z} = \frac{\partial \varphi_p}{\partial z} = 0$$

Under these conditions we can express the carrier densities in the whole volume by solving the continuity equations two–dimensionally in the middle of the channel width and by the following extension of this solution

$$n_{x,y,z} = n_{x,y,\frac{w}{2}} \cdot exp\left(-\frac{1}{U_t} \cdot (\Psi_{x,y,\frac{w}{2}} - \Psi_{x,y,z})\right) \tag{2.10}$$

$$p_{x,y,z} = p_{x,y,\frac{w}{2}} \cdot exp\left(+\frac{1}{U_t} \cdot (\Psi_{x,y,\frac{w}{2}} - \Psi_{x,y,z})\right) \tag{2.11}$$

The index $\frac{w}{2}$ denotes the middle of the channel width.
The second level of sophistication is obtained by assuming negligible current flow in the third dimension for the majorities and solving the continuity equation fully three–dimensional for the minorities.

The third level is the full three–dimensional continuity equation for both the minorities and the majorities.
With the above described model well established effects like channel narrowing, shift of threshold voltage and higher breakdown voltage at small channel width compared to large channel width can be simulated.

3 The numerical method

The fully adaptive automatic mesh refinement algorithm has been considerably improved to equidistribute the discretisation errors of the partial differential equations. The discretisation by standard finite differences in all three dimensions is more precisely descriped in [2]. The three coupled nonlinear difference equations are solved by Gummel's iterative method. The solutions of the linearized equations are obtained by the SOR method with an adaptive relaxation factor ω [5] for the Poisson equation while this relaxation factor is assumed constant and equal to 1.5 for the three–dimensional continuity equations. By some investigations saver and quicker convergency has been obtained. With a good guess of the start solution we got the final solution two times faster (including the time for getting the start solution) than without.

Using the SOR method, after small amount of work on the precondition matrix, the solution for $A \cdot x = b$ can be simplified in this method:

$$x_i^{(n+1)} = (1-\omega) \cdot x_i^{(n)} + \omega(b_i - \sum_j x_j^{(n+1)} a_j - \sum_k x_k^{(n)} a_k) \tag{3.1}$$

for $j < i$ and $k > i$ while $i = 1...NX \cdot NY \cdot NZ$.
Taking into account the special linearization algorithm of finite differences (with NX points in $x-$direction,NY points in $y-$direction and NZ points in $z-$direction) one can reduce (3.1) to:

$$\begin{aligned} x_i^{(n+1)} = (1-\omega) \cdot x_i^{(n)} + \omega(b_i - \\ - x_{i-1}^{(n+1)} a_{i-1} - x_{i-NX}^{(n+1)} a_{i-NX} - x_{i-NXY}^{(n+1)} a_{i-NXY} - \\ - x_{i+1}^{(n)} a_{i+1} - x_{i+NX}^{(n)} a_{i+NX} - x_{i+NXY}^{(n)} a_{i+NXY}) \end{aligned} \tag{3.2}$$

in which again $i = 1...NX \cdot NY \cdot NZ$.
For the Poisson equation there are two additional steps applied to improve the convergency. First we perform a subiteration of SOR in the channel region, so we can reduce the amount of unknowns essentially and improve the start solution. Second we introduce a second step for the SOR calculation [4] which can be written by use of (3.2) :

$$x_i^{(n+2)} = x_i^{(n-1)} \cdot \gamma^{(n)} + x_i^{(n+1)} \cdot (1 - \gamma^{(n)}) \tag{3.3}$$

γ is chosen as a factor depending on the iteration cycle and the total number of points.
$\gamma \propto \frac{1}{N}$ wherein N is the number of iteration cycles. By these improvements we obtained quicker and saver convergency even for ill conditioned problems.

4 Some results

In the following we will present some results calculated with the extended MINIMOS for a realistic MOSFET with $1\mu m$ x $1\mu m$ channel. By Fig. 1 the geometrical specifications of the MOSFET are given. The gate oxide thickness is $15nm$; the substrate doping is $2 \cdot 10^{16} cm^{-3}$.

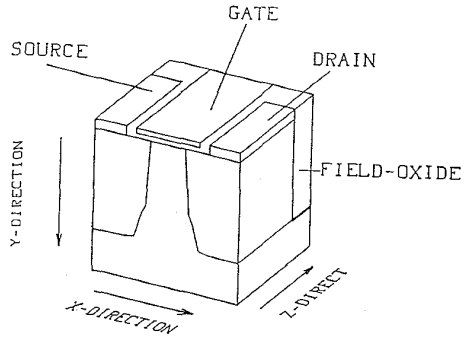

Fig.1: Perspective view of the three–dimensional MOSFET structure.

For detailed presentation we will choose two effects, first the threshold voltage and the channel narrowing, and second a new effect .

Threshold voltage

Three–dimensional simulation results using the extended MINIMOS are shown in Fig. 2 and 3. The bias conditions are $U_D = 2.0V, U_S = U_B = 0.0V$ and $U_{GS} = 0.73V$ which is close to the threshold voltage.

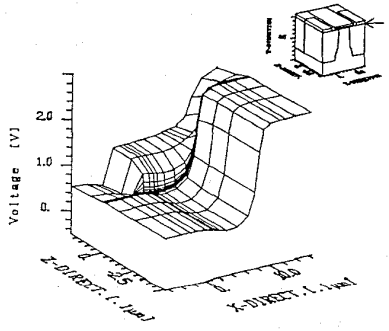

Fig.2: 3D–plot showing the surface potential at bias $U_{DS} = 2.0V, U_{BS} = 0.0V, U_{GS} = 0.73V$.

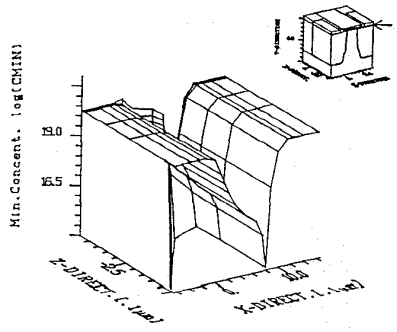

Fig.3: 3D–plot showing the minority density at bias $U_{DS} = 2.0V, U_{BS} = 0.0V, U_{GS} = 0.73V$.

The three–dimensional plot of the surface potential (Fig. 2) gives no direct insight why the threshold voltage should be higher for narrow channel devices than for wide, but one can easily see in Fig. 3 that the channel charge of the minorities (electrons in our case), which are responsible for the current, is lower than assumed in two–dimensional calculations. This effect is originated by the finite channel width. Thus for a given value of carrier density in the channel the gate voltage has

to be higher for a small channel device than for a wide one. The well known 'channel narrowing' results from the same reasons.

The new effect

Under certain bias conditions the 'channel narrowing' can change into its opposite so that at the channel edge an accumulation of minorities can be seen (Fig. 5). The bias voltages are assumed to be $U_D = 2.0V$,$U_S = U_B = 0.0V$ and $U_{GS} = 3.0V$. The corresponding three–dimensional plot of the surface potential is shown in Fig. 4.

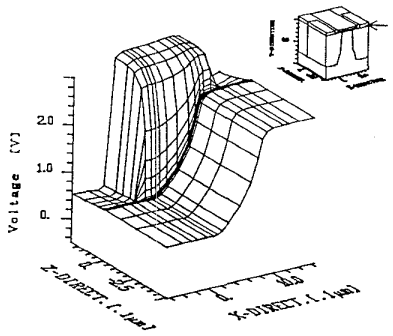

Fig.4: 3D–plot showing the surface potential at bias $U_{DS} = 2.0V$,$U_{BS} = 0.0V$,$U_{GS} = 3.0V$.

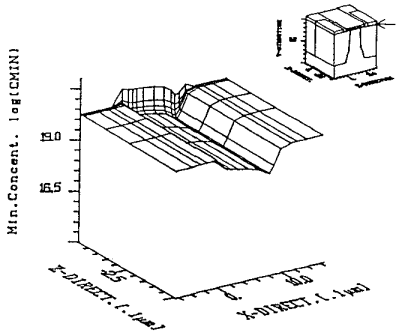

Fig.5: 3D–plot showing the minority density at bias $U_{DS} = 2.0V$,$U_{BS} = 0.0V$,$U_{GS} = 3.0V$.

This effect can be easily explained. If the gate voltage is very high the electric field in the field–oxide interface forces the electrons (in our case) to accumulate in this region. So we can observe a high current density at the channel edge which can also be seen in the $I_D - U_{GS}$ characteristics (Fig. 6). Of course this effect becomes much more important for smaller channel width.

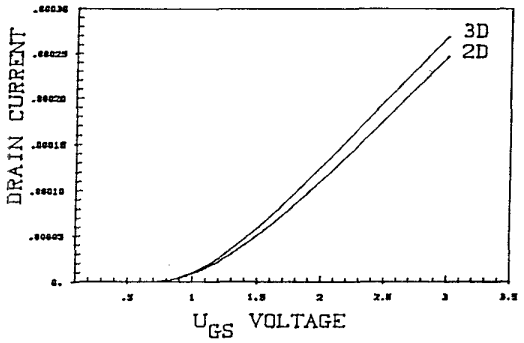

Fig.6: Characteristics of the simulated device I_D versus U_{GS}.

Acknowledgement

This work was supported by the research laboratories of SIEMENS AG at Munich, FRG, by

DIGITAL EQUIPMENT CORP. at Hudson, USA, and by the "Fonds zur Förderung der wissenschaftlichen Forschung", project S43/10. We are indepted to Prof. H. Pötzl for many helpful discussions.

References:

[1] S.Selberherr, The status of MINIMOS, Proc. Simulation of semiconductor devices and processes, pp 2-15, Swansea, 1986

[2] S.Selberherr, Analysis and simulation of semiconductor devices , ISBN 3-211-81800-6, Springer, WIEN NEW-YORK, 1984

[3] S.M.Sze,Physics of semiconductor devices, ISBN 0-471-09837-X, John Wiley & sons, 1981

[4] L.A.Hageman,Franklin T.Luk,David M.Young, On the equivalence of certain iterative acceleration methods, SIAM J.NUMER.ANAL., pp 852-873, vol. 17 No. 6, Dec 1980

[5] O.Axelsson,Solution of linear systems of equations;Iterative methods, Lecture notes in mathematics 574, SMT, 1976